Efficient Production of Clean Power and Hydrogen Through Synergistic Integration of Chemical Looping Combustion and Reforming

Mohammed N. Khan [1,2] , **Schalk Cloete** [3,*] **and Shahriar Amini** [1,3,*]

1   Department of Energy and Process Engineering, Norwegian University of Science and Technology, NO-7491 Trondheim, Norway; mohammednazeer.khan@vito.be
2   Separation and Conversion Technology Unit, Flemish Institute for Technological Research (VITO), 2400 Mol, Belgium
3   Process Technology Department, SINTEF Industry, NO-7465 Trondheim, Norway
*   Correspondence: schalk.cloete@sintef.no (S.C.); shahriar.amini@sintef.no (S.A.)

Abstract: Chemical looping combustion (CLC) technology generates power while capturing CO_2 inherently with no direct energy penalty. However, previous studies have shown significant energy penalties due to low turbine inlet temperature (TIT) relative to a standard natural gas combined cycle plant. The low TIT is limited by the oxygen carrier material used in the CLC process. Therefore, in the current study, an additional combustor is included downstream of the CLC air reactor to raise the TIT. The efficient production of clean hydrogen for firing the added combustor is key to the success of this strategy. Therefore, the highly efficient membrane-assisted chemical looping reforming (MA-CLR) technology was selected. Five different integrations between CLC and MA-CLR were investigated, capitalizing on the steam in the CLC fuel reactor outlet stream to achieve highly efficient reforming in MA-CLR. This integration reduced the energy penalty as low as 3.6%-points for power production only (case 2) and 1.9%-points for power and hydrogen co-production (case 4)—a large improvement over the 8%-point energy penalty typically imposed by post-combustion CO_2 capture or CLC without added firing.

1. Introduction

Anthropogenic carbon dioxide (CO_2) emissions to the atmosphere have risen beyond 415 ppm, causing climate change [1]. Due to this, the Paris Climate Accord has vowed to limit the global temperature rise below 2 °C of the pre-industrial level [2]. The conventional power generation technologies such as natural gas power plants (NGCC) suffer a considerable energy penalty when integrated with a carbon capture facility. An amine-based capture system reduces plant efficiency by ~8%-points [3] (all quoted efficiencies are LHV-based). Thus, the energy penalty is the primary cost driver for CO_2 capture technologies due to increased fuel costs and a greater amount of plant capital required to achieve a given electricity output. The increased fuel usage is also accompanied by increased emissions. Therefore, the development of novel energy conversion technologies with high CO_2 capture efficiency is essential.

Chemical looping combustion combined cycle power plants (CLC-CC) have the inherent capacity to capture CO_2 with a minimum penalty only required for compression [4]. The fuel and the oxidizer are treated separately using an oxygen carrier (OC), giving out a pure stream of CO_2 along with condensable water. The energy penalty is only for compressing the CO_2 to high pressures as well

as a minor penalty related to the reactor pressure drop. Ishida et al. [4] were one of the pioneers in analyzing CLC power generation systems and reported electrical efficiencies as high as 50.2%. In another study, Ishida and Jin [5] reported an exergy-based efficiency of 55.1% with the possibility of reaching 60% in the future with the advancement in power conversion and reactor operation. However, the CO_2 compression power is not accounted for, making this efficiency appear overly optimistic. Naqvi et al. [6] introduced the CO_2 compression system and reported the net electrical efficiency to be 52.2%. In a follow-up study, Naqvi and Bolland [7] used a multi-pressure CLC plant and reported a 0.8%-point improvement in electrical efficiency. In a similar study, Hassan et al. [8] reported the efficiencies to be as high as 52%. Zhu et al. [9] carried out a technical assessment on a CLC combined cycle plant using different OCs such as nickel, copper, and ilmenite. The net electrical efficiencies reported were 50.14%, 48.02%, and 45.59%, respectively. Ogidiama et al. [10] conducted a detailed technical assessment on natural gas-fired CLC combined cycle plant using NiO as the OC and reported the net electrical efficiency as 55.6%. Several other researchers reported electrical efficiencies ranging from 41.21–44.27% [11], 51–52% [12], 45.92–53.21% [13], and 52.04% [14].

These efficiency numbers are relatively low relative to those possible in modern natural gas-fired plants which can achieve efficiencies over 60%. This is mainly due to the low turbine inlet temperature (TIT) achieved in CLC processes [15] due to the OC material, reactor, and downstream particle filter operating temperature limitations. Due to this, the TIT of CLC systems is commonly modeled in the range of 800–1200 °C [16]. Operating the CLC plant beyond these temperatures will result in attrition, agglomeration, or thermal sintering of the material [16]. Temperature resistant OCs, especially for attrition, are being developed [17]. However, the CLC operating temperatures are currently difficult to match with the TIT of modern gas turbines, which can be as high as 1600 °C [18].

This problem is addressed by introducing an additional combustor downstream of the air reactor to raise the TIT, which in turn is dependent on combustor outlet temperature (COT). Either natural gas (NG) or hydrogen (H_2) can be burnt in the combustor in the presence of high-temperature O_2 depleted air from the AR. The improvement in electrical efficiency by introducing an additional combustor was studied in detail by Khan et al. [19]. The results showed a significant improvement in the electrical efficiencies by raising the COT to 1416 °C, which is typical of GE F-series gas turbines. When NG is used as fuel in the combustor, the electrical efficiency obtained was 55.31%, with an energy penalty of 2.9%-points compared to a NGCC plant. However, the burning of NG produces CO_2 in the combustor, which reduces the CO_2 avoidance of the plant. Therefore, burning H_2 is necessary to achieve high CO_2 avoidance rates. Khan et al. [19] also investigated the use of H_2 in the combustor at different H_2 production and CO_2 capture efficiencies ranging from conventional to more advanced H_2 production scenarios. For the most advanced scenario with H_2 production and CO_2 capture efficiencies of 90% and 100%, respectively, the electrical efficiency was reported to be 53.64% with an energy penalty of 4.5%.

However, the current H_2 production processes are also accompanied by CO_2 emissions. Therefore, the source of H_2 is critical in achieving high efficiencies with maximum CO_2 capture. Conventional steam-methane reforming (SMR) is about 70% efficient (H_2 LHV output/NG LHV input) with 80% carbon capture when using an amine-based capture system. This increases the H_2 cost by 40–100% [20]. Another promising method is chemical looping reforming (CLR) which reduces the cost of H_2 significantly [21]. The attractiveness of the CLR process can be enhanced by using palladium-based (Pd) membranes with high H_2 selectivity. The membranes are used to extract H_2 directly from the reforming reactor, which eliminates the need for water-gas shift and pressure swing adsorption units for separation. Spallina et al. [22] conducted an economic assessment of such a system and estimated that the H_2 production cost can be well below that of a conventional SMR plant without CO_2 capture. This concept has also been demonstrated at laboratory scale [23]. Operating these systems at high pressures is possible and thus the energy penalty in CO_2 compression can be further reduced.

The current study presents the efficiency improvement strategies by integrating the CLC plant with an additional combustor with the membrane-assisted chemical looping reforming (MA-CLR) plant. With proper heat integration, as described in the next section, the electrical efficiencies are

expected to reach beyond that reported by Khan et al. [19]. Therefore, five cases with different degree of plant integration are investigated in the present study. The process integration of these two plants also presents the opportunity of plant flexibility in producing either electricity or both electricity and H_2. Out of the five cases, two are developed based on the plant flexibility feature. The plant performances are estimated in terms of efficiencies such as electrical, H_2 production, and CO_2 capture and avoidance. Results will be compared with the NGCC combined cycle plant presented in our previous work [19].

2. Description of the Concept Working Principle

The principle behind the power and hydrogen production processes presented in this study is simply illustrated in Figure 1, where the red arrows indicate the two key points of integration between the CLC and CLR processes. As mentioned earlier, the reason for additional firing with hydrogen is to raise the temperature in the stream going to the gas turbine beyond that which is achievable in the CLC reactors, thus increasing power cycle efficiency. However, if SMR hydrogen production with conventional CO_2 capture is used for this added firing, the gains from higher power cycle efficiency are canceled out completely by the low efficiency of hydrogen production with CO_2 capture [19]. Therefore, the use of a highly efficient clean hydrogen production process is needed.
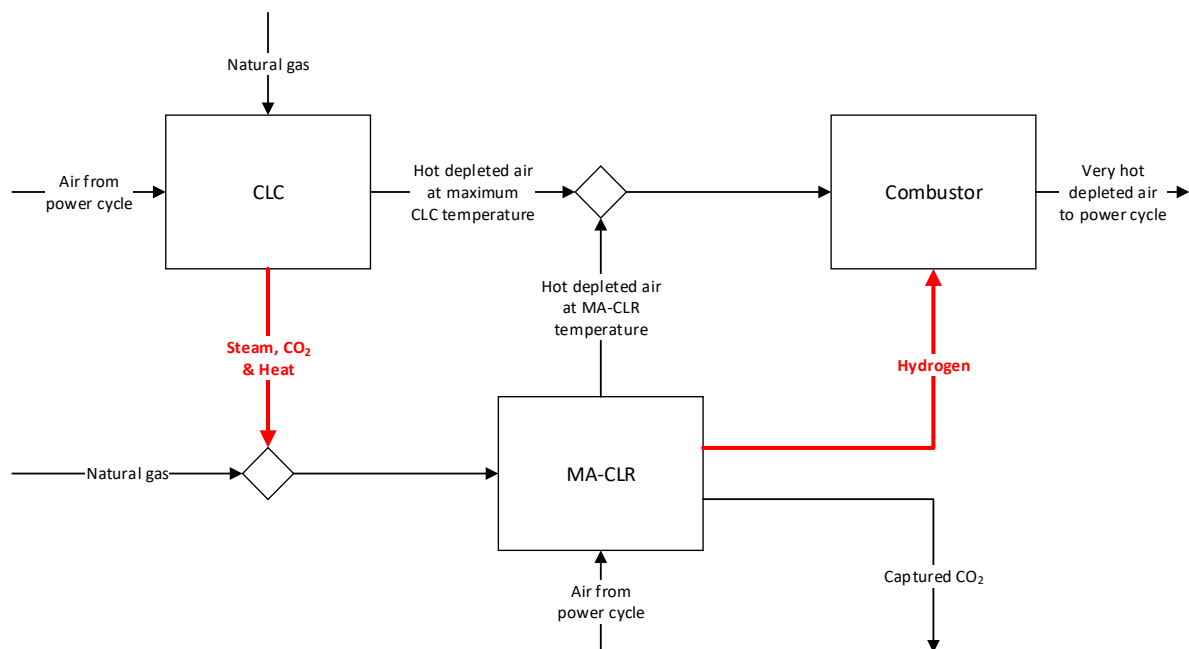

Figure 1. Simplified illustration of the working principle behind the plants described in this study.

The primary energy penalty in hydrogen production with CLR-based processes is the provision of the steam required for NG reforming. When the produced hydrogen is combusted in a gas turbine, all the energy required to raise the steam in the hydrogen production process is lost because the condensation enthalpy of the steam resulting from hydrogen combustion cannot be converted to useful work. Nazir et al. [24] reported that this steam-related penalty accounts for about 5.8%-points of the 7.2%-point energy penalty of a combined cycle power plant fired by hydrogen from a gas switching reforming (GSR) process, illustrating the importance of this energy penalty. GSR works on the CLR principle, only keeping the oxygen carrier in a single reactor with switching valves to alternately expose it to different gases.

The key novelty in the present study is the use of steam and heat in the CLC fuel reactor outlet stream to minimize this energy penalty. An important thermodynamic advantage of the CLC concept is that the steam resulting from the reduction reaction in the CLC fuel reactor along with the CO_2 can be obtained at high pressures. The condensation enthalpy of this steam could be recovered at useful

temperatures (150–200 °C), whereas it would be lost in the conventional NGCC plant where the water vapor in the flue gas condenses around room temperature. Thus, the integration of the CLC process presents the opportunity to recover and productively utilize this latent heat.

Therefore, the main objective of the present work is to devise and compare different process integration options for efficiently utilizing the steam and heat in the CLC fuel reactor outlet gases for hydrogen production in the MA-CLR process. This principle can be applied to the integration of any NG reforming process where steam is required, but the MA-CLR process was selected for use in this study based on the promising techno-economic performance reported in Spallina et al. [22].

3. Methodology

3.1. Plant Configurations

A conventional NGCC plant developed in our previous work [19] is used as a benchmark for comparing the results obtained in this study. The NGCC plant and all the other models are developed based on the recommendations of the European benchmarking task force (EBTF) report [25]. In an NGCC plant, fuel is preheated and the air is compressed before supplying to the combustor. The hot flue gases are expanded to produce power and sent to steam cycle for heat recovery. The F-class gas turbine system GE 9371FB with a COT of 1416 °C has been considered due to the robust design and fuel flexibility [25]. A triple pressure single reheat heat recovery steam generator (HRSG) is considered for steam generation from recovered heat. The steam is expanded in steam turbine (ST) and cooled down in condenser (COND) and cooling tower (CT). The entire steam cycle is simulated in Thermoflex [26] while the other equipment are modeled in Aspen Plus [27]. The main assumptions are taken from the EBTF report [25] and are given in Table 1.

Figure 2 shows a schematic of a CLC combined cycle plant with an additional combustor and the arrangements for combustor fuel supply, steam injection, and exhaust gas recirculation for NOx control. The plant specifications are similar to the conventional CLC cycle without added firing. A nickel-based OC (NiO) supported on $NiAl_2O_4$ is supplied to the fuel reactor (FR) where the endothermic reduction reaction produces CO_2 and H_2O. The reduced OC is re-oxidized in the air reactor (AR) in an exothermic reaction with air. The O_2 depleted air from the AR is passed through an expander to produce power and sent to HRSG for heat recovery. The CO_2 stream is also expanded and is further used to preheat the incoming fuel followed by condensation of steam and CO_2 compression to high pressures (supercritical state). The operating conditions of this plant are taken from the work of Naqvi and Bolland [7]. More details about this plant, including stream information, can be found in our previous work [19].

This conventional CLC plant is fitted with an added combustor to raise the COT to match the reference NGCC plant. The H_2 is compressed to about 1.5 times the oxidizer (O_2 depleted air) pressure and injected into the combustor. The O_2-depleted air from the AR is considered as the oxidizer in the combustor where its temperature is raised from 1160 °C to 1416 °C. The Gibbs energy minimization concept is considered in solving the heat and mass balances. As a result, the air reactor exhaust temperature of 1160 °C is obtained for the same inlet operating conditions. Such a simplified reactor modeling assumption is merited by the high reactivity of the Ni-based oxygen carrier employed. Given the limitations to the thermal stability of the oxygen carrier material, the temperature obtained in the air reactor is more conservative. It should be noted that higher CLC operating temperatures pose problems in solid handling such as sintering and agglomeration. The plant main assumptions are given in Table 1 and are also taken from the EBTF report [25].

The source of H_2 in Figure 2 is the MA-CLR plant represented in Figure 3. The NG is preheated to 324 °C before subjecting to desulfurization to convert any sulfur compounds. Then the steam is mixed with the NG to result in a steam/carbon ratio of 2, which is slightly higher than the ratio of 1.75 used by Spallina et al. [22] to ensure good methane conversion and no carbon deposition. The mixture is then pre-reformed using a nickel-based catalyst to convert higher hydrocarbons at 490 °C for minimizing coke formation in the MA-CLR reactor. Then the pre-reformed gas is further heated before entering

the fuel reactor of the MA-CLR plant. As shown in Figure 3, the FR contains Pd-membranes for H_2 extraction. In this process, the same OC ($NiO-NiAl_2O_4$) is used, which also acts as the catalyst for reforming and water-gas shift reactions. The retentate stream (CO_2 and H_2O) comes out of the reactor from the top while the permeate stream consisting of pure H_2 is extracted through the membranes. The plant specifications are listed in Table 1 and more details, includeing stream information, can be found in our previous work [28].

Table 1. Plant specifications and main assumptions.

Unit	Specification
Natural gas (vol. %)	CH_4—89%; C_2H_6—7%; C_3H_8—1%; C_4H_{10}—0.11%; CO_2—2%; N_2—0.89% (70 bar and 15 °C)
Air composition (vol. %)	N_2—77.3%; O_2—20.7%; H_2O—1%; Ar—0.92% (1.013 bar and 15 °C)
Hydrogen supply, (°C/bar)	15/14
LHV-NG/H_2, (kJ/kg)	46,502/119,800
Reactor/Combustor pressure drop, % of inlet pressure	5%
Air/H_2 compressor polytropic efficiency	92%
Gas/CO_2 turbine polytropic efficiency	92/85%
Compressors/turbines isentropic efficiency	85%
Mechanical efficiency	98%
MA-CLR	
Pre-reforming temperature, (°C)	490
Steam-to-carbon ratio	2
Reforming pressure, (bar)	20
Permeate pressure, (bar)	4 (all cases)/6 (case 5)
Final H_2 condition, (°C/bar)	30/150
Steam cycle (HRSG)	
Steam turbine system	Condensing reheat steam turbine
Reheat temperature, (°C)	Depends on each case
HP/IP/LP steam turbine isentropic efficiency	Depends on steam conditions and turbine size
HP/IP/LP steam pressure, (bar)	124/18.3/3.4
HP/IP/LP steam temperature, (°C)	Depends on each case
Pinch temperature/Approach temperature, (°C)	15/5
Condenser pressure, bar	0.048–0.067 (depends on each case)
Cooling system	Water cooling with natural draft cooling tower
Water pump efficiency	70%
Heat Exchangers	
Minimum temperature approach, gas-gas/gas-liquid, (°C)	10/10
Pressure drop, % of inlet pressure	1%
CO_2 compression	
Compression stages	3
Compression ratio per stage	4.31
Final CO_2 condition, (°C/bar)	30/110
Compressor stages isentropic efficiency	80/80/75%
CO_2 pump efficiency	75%

In the current study, five cases with different degrees of integration between the CLC plant shown in Figure 2 and the MA-CLR plant shown in Figure 3 are investigated (Table 2). All cases feature added combustion of hydrogen after the CLC reactors and the cases are arranged in order of increasing integration between the CLC and MA-CLR processes. Case 1 is the direct integration of the CLC and MA-CLR process by connecting the H_2 supply line to the combustor.

Case 2 has additional integration as shown in Figure 4. In this configuration, some part of the fuel reactor outlet stream of the CLC system is mixed with the NG required in the MA-CLR system maintaining steam-to-carbon ratio 2. This has the advantage of replacing the steam that normally needs to be raised for hydrogen production in the MA-CLR process with steam resulting from the combustion of NG. Just enough CLC fuel reactor flue gases are used to supply the steam required to produce enough hydrogen for the added combustor. The outlet stream from the AR of MA-CLR is expanded in the turbine followed by preheating the feed water. The retentate stream is used to produce saturated steam and then sent for compression whereas the permeate stream is used to superheat the steam, which is then sent to the HRSG. The permeate is then used to further preheat the feed water

before it is compressed and sent to the combustor. Since the CO_2 stream is at 20 bar pressure, it is introduced in the CO_2 compression process after the second stage.
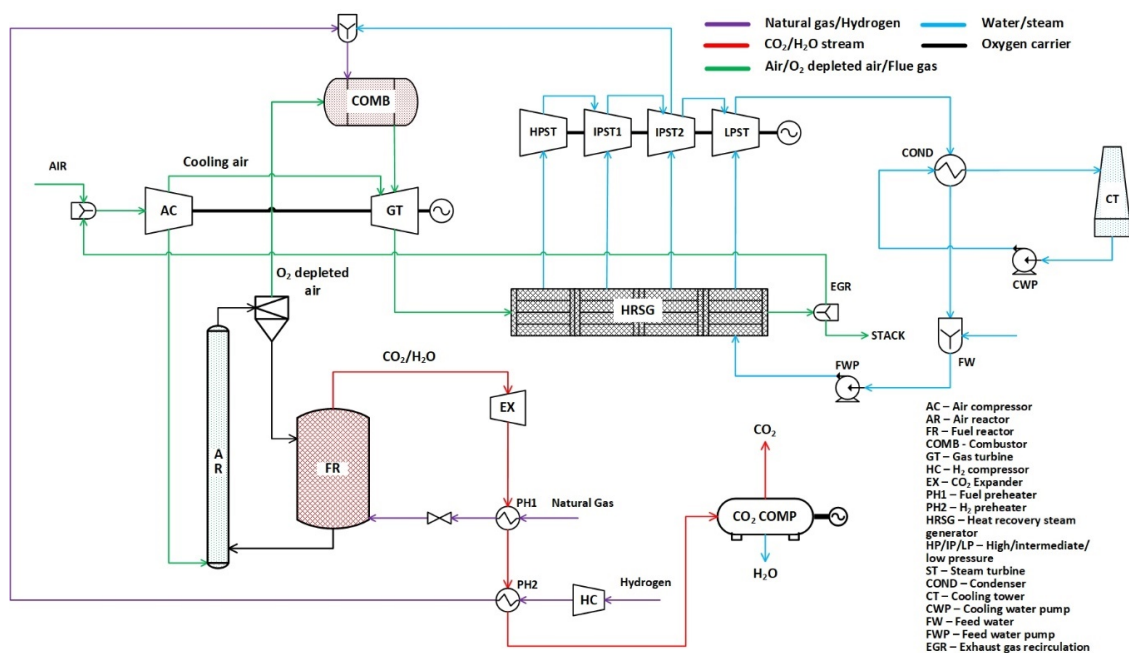

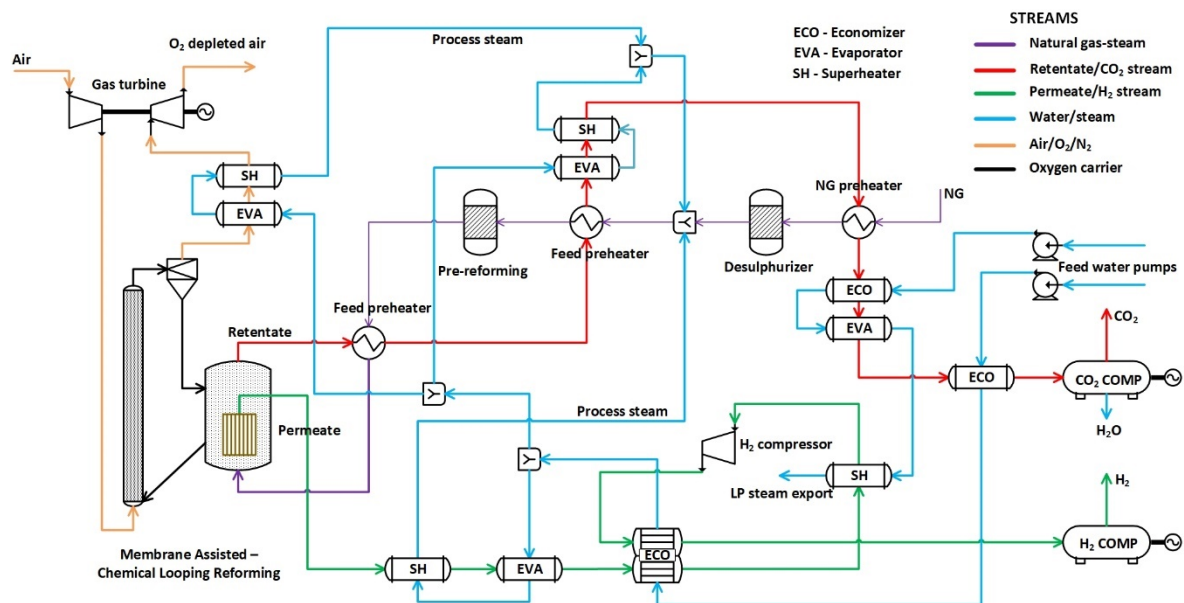**Figure 2.** Schematic of CLC plant with an additional combustor [19].

Figure 3. Schematic of membrane-assisted chemical looping reforming (MA-CLR) plant [28].

Table 2. Summary of the CLC and MA-CLC integrations investigated in this study.

| Case #	Description
Case 1	A simple integration where H_2 from MA-CLR is fed to the added combustor after the CLC reactors.
Case 2	Case 1 with an additional coupling by using part of the CLC fuel reactor flue gas as a steam source for reforming in MA-CLR.
Case 3	Using all the CLC fuel reactor flue gas as a steam source for reforming in MA-CLR and producing excess H_2 for export.
Case 4	Combining CLC and MA-CLR into a single reactor unit and using a 2-phase flow heat exchanger to raise steam from the steam condensation enthalpy in the fuel reactor outlet stream.
Case 5	Case 4 produces excess H_2 and Case 5 was formulated to produce only power by sweeping the membranes with additional steam to extract more heat from the reactor.
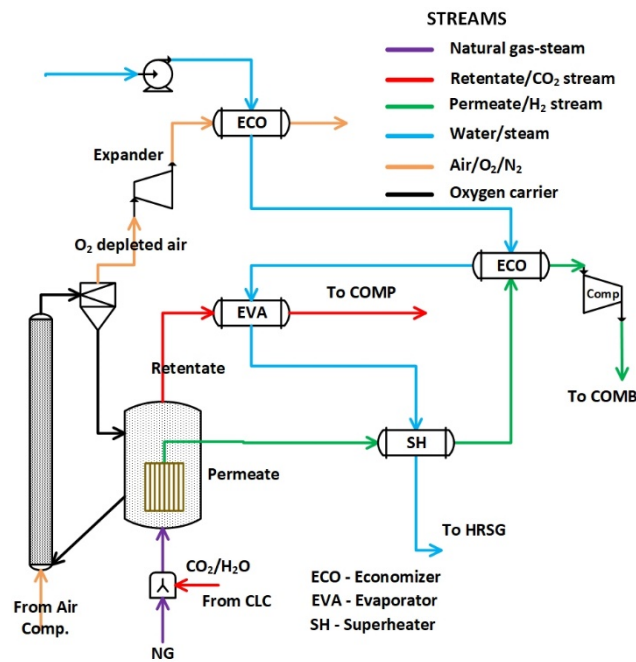
Figure 4. Schematic of case 2 (only the MA-CLR is shown).

　　Case 3 is shown in Figure 5. In this case, the whole fuel reactor outlet stream of the CLC plant is mixed with NG and injected into the fuel reactor of MA-CLR. Hence, the CO_2 expander is not included in this configuration. A large amount of steam from the CLC fuel reactor means that more H_2 is produced than that required in the combustor. Additional H_2 is compressed to high pressure (HP) and exported. Both the air reactor outlet streams of CLC and MA-CLR are mixed and sent to the combustor. This is done to further simplify the process by eliminating the expander used in the MA-CLR process. The AR outlet stream from the MA-CLR plant is no longer used for steam generation purpose, rather it is fed to the combustor where more H_2 can be burnt to produce more power (in absolute terms) and subsequently recover more heat in the steam cycle. The retentate stream is used to produce saturated steam and preheats part of feed water whereas the permeate stream is used to superheat the steam followed by preheating the rest of the feed water.

　　Cases 4 and 5 combine the CLC and MA-CLR reactors into a single unit for greater process intensification by increasing the air flowrate and temperature of the MA-CLR air reactor to CLC levels. Since a large fraction of the methane fed to the membrane reactor must be combusted in this configuration, a large amount of fuel must slip past the membranes to reduce the oxygen carrier, allowing a smaller membrane surface area concentrated in the lower reactor regions where H_2 partial pressures are high. Relative to cases 2 and 3, cases 4 and 5 also avoid the feed of CO_2 in the CLC fuel reactor stream to the membrane reactor, thereby shifting the equilibrium reactions further towards greater H_2 production, allowing additional reductions in the required membrane surface area. A future economic assessment with more detailed reactor modeling will be required to quantify these benefits.

　　In case 4 (Figure 6), the NG is cooled after desulphurization before being mixed with liquid water pumped at 19 bar to maintain a steam-to-carbon ratio of 2. The mixture is sent to a two-phase heat exchanger (2P-HX). This gas-liquid mixture (stream 4 in Figure 6) allows the water to start evaporating at low temperatures so that the condensation enthalpy from the steam in the retentate stream (CO_2 stream) exiting the FR can be used to efficiently raise this steam, effectively granting access to the HHV of the NG (~10% greater than the LHV). The retentate stream is also used to preheat the water to 114 °C before compression to a supercritical state. The NG-steam mixture is fed into the FR of the MA-CLR plant. This reactor configuration with the membranes is the same as discussed above. The permeate stream consisting of pure H_2 exits at 700 °C and is used to generate HP superheated steam (stream 21, Figure 6), which is supplied to the HRSG for power generation. The required amount of H_2 in

the combustor to maintain the COT of 1416 °C is split from the permeate stream (stream 12, Figure 6), with the remainder being compressed to storage pressure. The split H_2 is burnt in the combustor with an AR exhaust stream as the oxidizer to power the gas turbine and downstream heat recovery in the steam cycle.
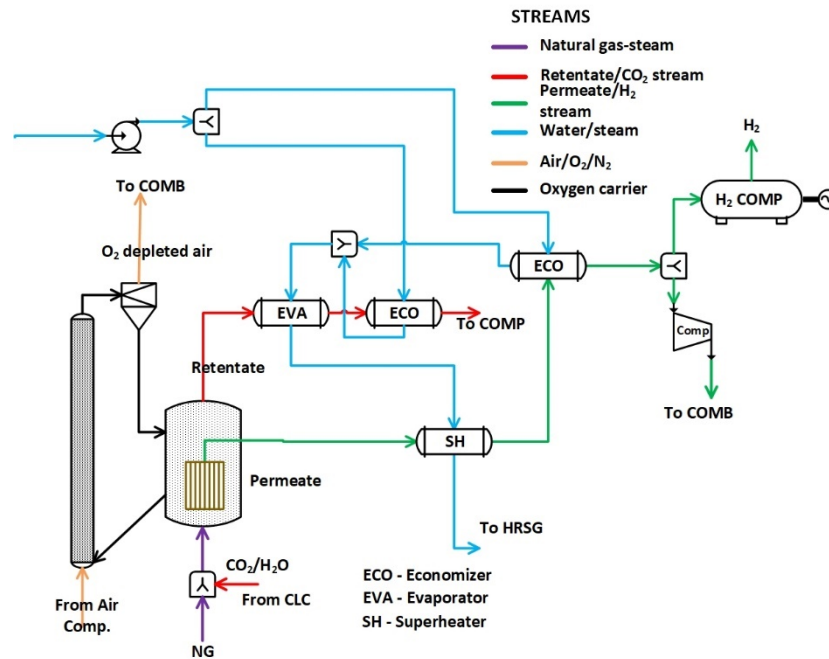

Figure 5. Schematic of case 3 (only MA-CLR is shown).

Table 3. Stream data of case 4 with 2P-HX (mainly H_2 production) in Figure 6.

St.	T	P	Mass Flow	Mole Composition (%)							
	°C	bar	kg/s	CH_4	C_{2+}	N_2	O_2	CO_2	H_2O	Ar	H_2
1	10.0	70.0	17.0	89	8.11	0.89	0	2	0	0	0
2	236.0	69.3	17.0	89	8.11	0.89	0	2	0	0	0
3	301.5	19.4	17.0	90.83	6.28	0.89	0	2	0	0	0
4	25.3	19.2	53.2	29.03	2.01	0.28	0	0.64	68.04	0	0
5	220.0	19.0	53.2	29.03	2.01	0.28	0	0.64	68.04	0	0
6	700.0	18.1	72.3	0	0	0.33	0	40.41	59.26	0	0
7	672.1	17.9	72.3	0	0	0.33	0	40.41	59.26	0	0
8	105.2	17.5	72.3	0	0	0.33	0	40.41	59.26	0	0
9	38.4	110.0	45.2	0	0	0.81	0	99.04	0.15	0	0
10	700.0	4.0	4.9	0	0	0	0	0	0	0	100
11	159.7	3.9	4.9	0	0	0	0	0	0	0	100
12	89.6	3.8	4.9	0	0	0	0	0	0	0	100
13	30.0	150.0	4.5	0	0	0	0	0	0	0	100
14	15.0	1.0	161.3	0	0	77.39	20.74	0.03	1.01	0.83	0
15	440.5	20.0	161.3	0	0	77.39	20.74	0.03	1.01	0.83	0
16	1416.4	18.1	137.7	0	0	87.61	6.33	0	5.04	1.02	0
17	654.9	1.0	137.7	0	0	87.61	6.33	0	5.04	1.02	0
18	15.0	1.0	13.9	0	0	0	0	0	100	0	0
19	114.0	128.4	13.9	0	0	0	0	0	100	0	0
20	327.3	127.1	13.9	0	0	0	0	0	100	0	0
21	500.0	125.8	13.9	0	0	0	0	0	100	0	0

Case 4 produces a large amount of steam from the 2-phase flow heat exchanger, which leads to a lot of hydrogen production. It is therefore primarily a hydrogen production plant with some power

production. Therefore, case 5 (Figure 7) is devised for power production only, implying that the whole permeate H_2 (stream 12, Figure 7) is burnt in the combustor.
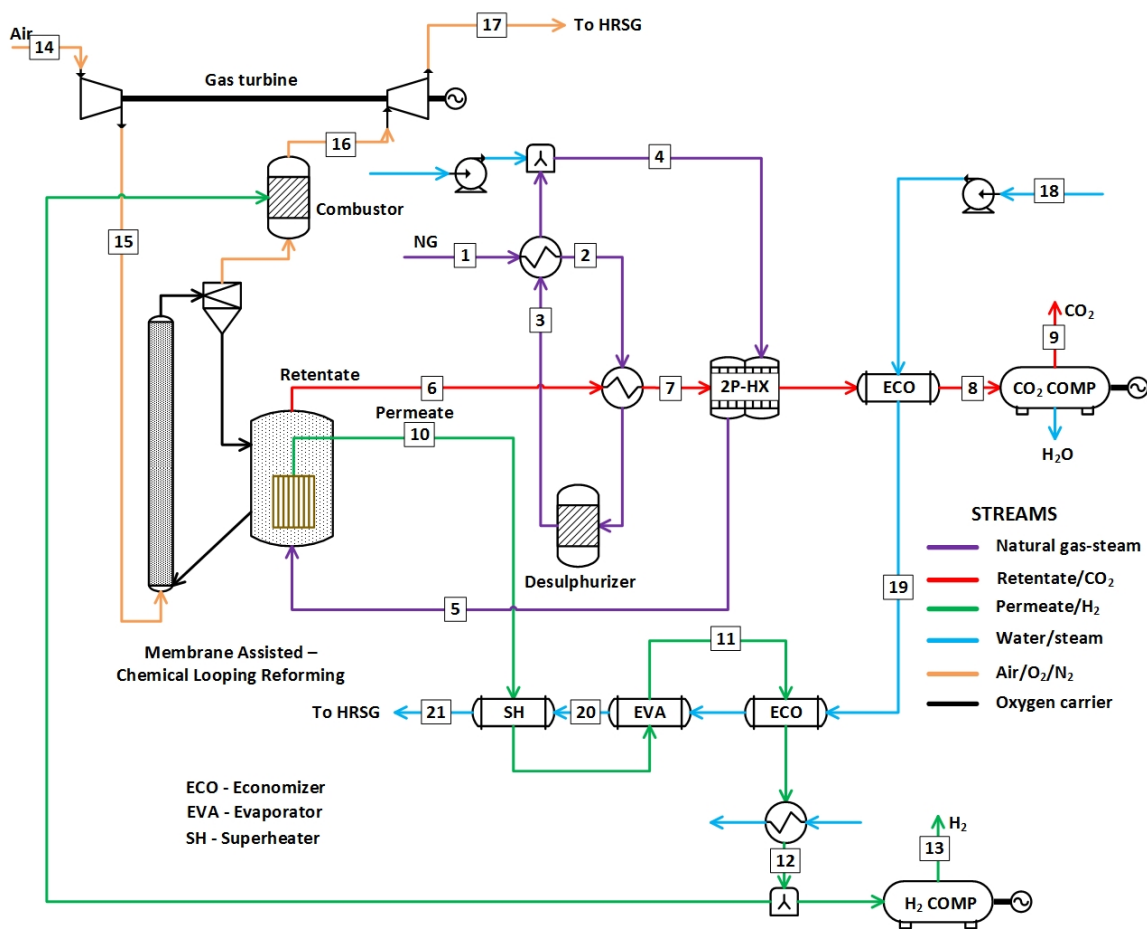

Figure 6. Schematic of case 4 (part H_2 is used in combustor). Stream numbers refer to stream details listed later in Table 3.

Table 4. Stream data of case 5 with 2P-HX (power production) in Figure 7.

| St.	T	P	Mass Flow	Mole Composition (%)							
	°C	bar	kg/s	CH$_4$	C$_{2+}$	N$_2$	O$_2$	CO$_2$	H$_2$O	Ar	H$_2$
1	10.0	70.0	17.0	89	8.11	0.89	0	2	0	0	0
2	236.0	69.3	17.0	89	8.11	0.89	0	2	0	0	0
3	301.5	19.4	17.0	90.83	6.28	0.89	0	2.00	0	0	0
4	25.3	19.2	53.2	29.03	2.01	0.28	0	0.64	68.04	0	0
5	650.0	19.0	53.2	29.03	2.01	0.28	0	0.64	68.04	0	0
6	700.0	18.1	98.7	0	0	0.21	0	25.61	74.18	0	0
7	681.6	17.9	98.7	0	0	0.21	0	25.61	74.18	0	0
8	160.1	17.5	98.7	0	0	0.21	0	25.61	74.18	0	0
9	38.4	110.0	45.2	0	0	0.81	0	99.04	0.15	0	0
10	700.0	6.0	9.5	0	0	0	0	0	30.13	0	69.87
11	209.1	5.9	9.5	0	0	0	0	0	30.13	0	69.87
12	484.3	28.5	9.5	0	0	0	0	0	30.13	0	69.87
13	15.0	1.0	672.3	0	0	77.39	20.74	0.03	1.01	0.83	0
14	440.5	20.0	672.3	0	0	77.39	20.74	0.03	1.01	0.83	0
15	1416.5	18.1	634.3	0	0	79.38	12.68	0	7.01	0.92	0
16	660.2	1.0	634.3	0	0	79.38	12.68	0	7.01	0.92	0
17	15.0	1.0	7.5	0	0	0	0	0	100	0	0
18	154.0	110.0	7.5	0	0	0	0	0	100	0	0
19	550.0	108.9	7.5	0	0	0	0	0	100	0	0
20	253.5	6.0	7.5	0	0	0	0	0	100	0	0
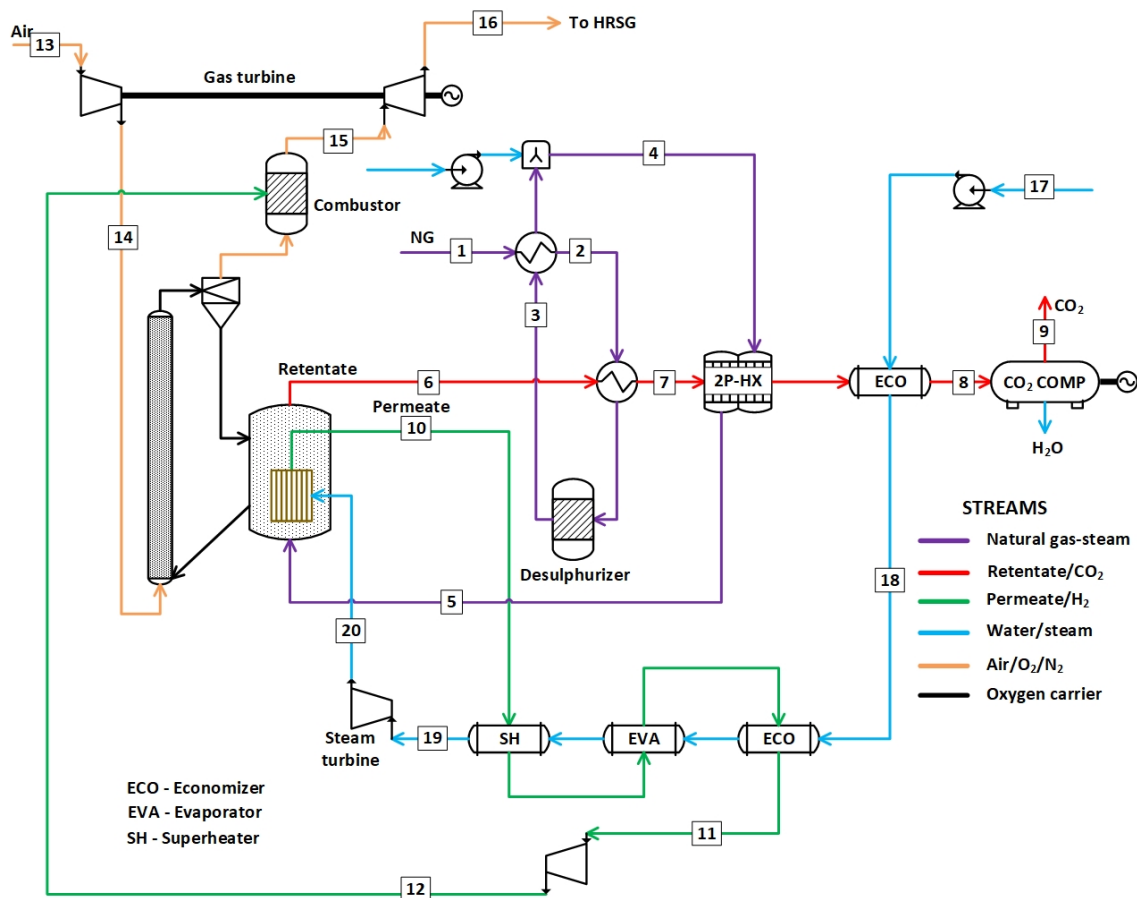
Figure 7. Schematic of case 5 (all H_2 is used in combustor). Stream numbers refer to stream details listed later in Table 4.

The main difference is that the HP superheater steam (stream 19, Figure 7) is expanded in a steam turbine and used as a sweep gas in the membranes. In this way, the steam is heated to the COT, requiring more heat production at the expense of hydrogen production. The amount of steam used in the sweep is adjusted so that the balance between heat and hydrogen production is just right to reach the specified COT when all the produced H_2 is fed to the combustor. An additional benefit is that the steam sweep lowers the partial pressure of H_2 in the membranes, increasing the driving force for H_2 permeability. This was accounted for by increasing the permeate pressure to 6 bar in this case.

3.2. Process Modeling and Plant Performance Indicators

Thermodynamic equilibrium is considered while solving the mass and energy balances in all the equipment. The property method, Redlich-Kwong-Soave equation of state with Boston-Mathias alpha function (RKS-BM), is used as it is recommended for hydrocarbons and applications involving light gases such as CO_2 and H_2 [29]. For the CLC plant, the reactors and the combustor are modeled using the reactor based on Gibbs energy minimization (RGIBBS) module in Aspen Plus [27], which assumes chemical and phase equilibrium. Perfect solid and gas separation is assumed and is done by using a cyclone block at the AR exit and a separator block at the FR exit. The efficiencies of the air/H_2 compressors, the gas turbine, and the expander are evaluated using a polytropic with the gas processors suppliers association (GPSA) method [30].

For the MA-CLR plant, a simple zero-dimensional (0D) mass and energy balance model is used to determine the reactor behavior, implying that no internal species or temperature profiles are resolved in the reactor. The temperature-dependent enthalpies of the gases were taken from the JANAF thermochemical database [31]. The results of this model are coupled with the process simulations.

The main assumptions used in developing the models are listed in Table 1. The model is solved to estimate the required air and the composition of the O_2 depleted stream from the MA-CLR AR (assuming complete O_2 conversion). Furthermore, the flowrate of the ultra-pure H_2 at the membrane outlet and the composition of the CO_2 rich stream at the MA-CLR FR outlet (assuming complete fuel conversion) are also obtained.

As mentioned earlier, the steam cycle consisting of a condensing reheat steam turbine system and HRSG was modeled in Thermoflex [26]. The reheat and the HP/IP/LP steam temperatures adjust automatically depending on the heat recovery in each case. Similarly, the efficiencies of the steam turbine and the condenser pressure varied depending on the stream conditions and turbine size required. A natural draft cooling tower system is considered for the condenser and inter-stage compressor cooling.

The plant performance of all the cases in the present study is evaluated by using net electrical efficiency (%), hydrogen production efficiency (%), efficiency penalty (%-points), CO_2 capture efficiency (%), and CO_2 avoidance (%) as shown below. The efficiency penalty is expressed using the global efficiency (Equation (6)) of the CCS plants to accurately reflect the performance of the plants with power and H_2 co-production:

$$\text{Net electrical efficiency}: \quad \eta_{net} = \frac{\dot{W}_{net}}{\dot{m}_{NG} \times LHV_{NG}} \tag{1}$$

$$\text{Hydrogen production efficiency}: \quad \eta_{H2} = \frac{\dot{m}_{H_2} \times LHV_{H_2}}{\dot{m}_{NG} \times LHV_{NG}} \tag{2}$$

$$\text{Efficiency penalty}: \quad \eta_{pen} = \eta_{net,\, ref} - \eta_{net,\, global,CCS} \tag{3}$$

$$\text{CO}_2 \text{ capture efficiency}: \quad \eta_{cap} = \frac{CO_2 \; captured}{CO_2 \; produced} \tag{4}$$

$$\text{CO}_2 \text{ avoidance}: \quad \eta_{avoid} = \frac{(CO_2 \; emitted)_{NGCC} - (CO_2 \; emitted)_{CCS}}{(CO_2 \; emitted)_{NGCC}} \tag{5}$$

For the cases with both power and H_2 generation (cases 3 and 4), the electrical and H_2 global efficiencies are defined as follows. The overall efficiency is the net efficiency of the plant as shown in Equation (8):

$$\text{Electrical global efficiency}: \quad \eta_{net,\, global} = \frac{\eta_{net}}{1 - \frac{\eta_{H_2}}{0.8}} \tag{6}$$

$$\text{H}_2 \text{ global efficiency}: \quad \eta_{H_2,\, global} = \frac{\eta_{H_2}}{1 - \frac{\eta_{net}}{0.58}} \tag{7}$$

$$\text{Overall efficiency}: \quad \eta_{overall} = \frac{\dot{W}_{net} + \dot{m}_{H_2} \times LHV_{H_2}}{\dot{m}_{NG} \times LHV_{NG}} \tag{8}$$

In these equations, η is the efficiency (%), $\dot{W}$ is the net power produced (kW), $\dot{m}$ is the fuel/H_2 mass flow (kg/s), LHV is the fuel/H_2 lower heating value (kJ/kg), and E is the emissions intensity (kg/kWh). The subscript *ref* stands for reference plant and *CCS* stands for the different CO_2 capture plants considered. The global efficiencies are the equivalent efficiencies calculated based on the fuel used for either electricity or H_2 production i.e., fuel used for H_2 or electricity is deducted from the total fuel input in their respective equations. The reference plant efficiencies for H_2 production and power generation were selected for an SMR plant (η = 80%) and NGCC plant (η = 58%), respectively.

4. Results and Discussion

The main results for power production from the different plant configurations are shown in Figure 8 with a power breakdown provided in Figure 9. As a reference, the net electrical efficiency of

the NGCC plant is 58.17%. It is also noted that, with an absorption post-combustion CO_2 capture plant (not modeled in this study), the energy penalty is around 8 %-points as reported in the literature [32]. This reference plant would achieve about 90% CO_2 capture, whereas the CO_2 capture efficiency and avoidance are almost 100% in all the cases considered in this study, assuming perfect loop-seal performance. Real systems may show lower CO_2 capture ratios if loop seals are not 100% effective.
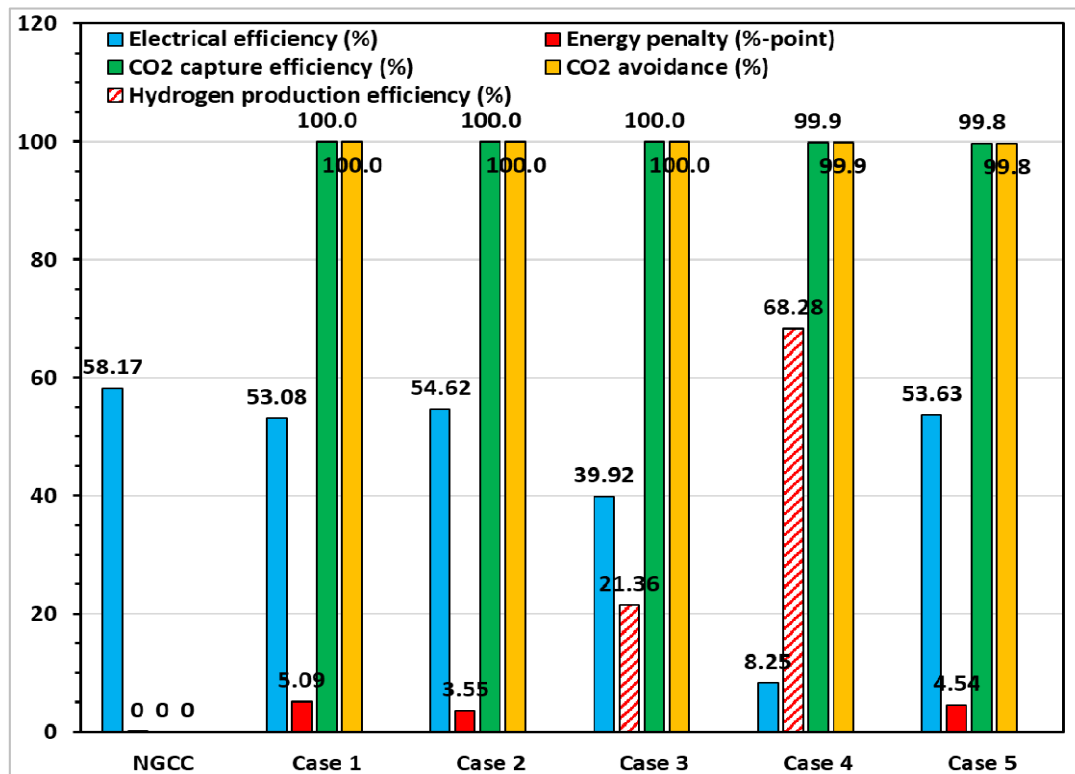

Figure 8. Performance comparison of different plant integration cases.

The net electrical efficiency of a conventional CLC combined cycle plant is 49.39% [19], which is slightly below the NGCC plant with conventional CO_2 capture. As outlined in the introduction, this relatively poor CLC performance can be improved by added firing with efficiently produced hydrogen, as is the focus of the present study.

In case 1, the added firing of the CLC plant with an additional combustor is done with hydrogen from a standalone MA-CLR plant. As shown in Figure 8, the net electrical efficiency of this configuration is 53.08% with an energy penalty of 5.09%-points. This is a substantial improvement when compared with the conventional CLC combined cycle plant and the NGCC plant with CO_2 capture. As shown in Figure 9, the combined power output from the gas turbine, steam turbines, and CO_2 expander in case 1 is about 2%-points lower than the reference plant. This is due to the less efficient power production (expansion at lower temperatures) of the CO_2 stream from CLC and the N_2 stream from MA-CLR. Most of the remaining 3%-points of efficiency penalty come from CO_2 compression after the CO_2 expander and H_2 compression before the added combustor. Thus, by simply utilizing efficiently produced H_2 in the added combustor, without any additional heat integration, the energy penalty can be reduced substantially relative to conventional CO_2 capture, while capturing all produced CO_2. In comparison, most of the energy penalty in post-combustion capture (PCC) system (~8%-points [33]) stems from using LP steam in regenerating the solvent that would have been used for power generation. This energy intensive step is avoided in CLC systems. Moreover, raising the TIT of such systems using an additional combustor improves the gas turbine efficiency. Hence, the overall improvement by firing H_2 from a highly efficient source is about 3.7%-points when compared to conventional CLC plant that operates at a lower TIT. Furthermore, the CO_2 capture efficiency from a PCC system is generally

90%, and higher CO_2 capture rates will increase the energy penalty significantly due to equilibrium constraints. Thus, achieving almost 100% capture with very high purity in these systems demonstrates that the energy consumption per kilogram of CO_2 capture will be lower. In addition, the electrical energy for compression is 0.32 MJ/kg-CO_2 as opposed to 0.43 MJ/kg-CO_2 in a PCC system [34] because the MA-CLR plant produces CO_2 already at elevated pressures.
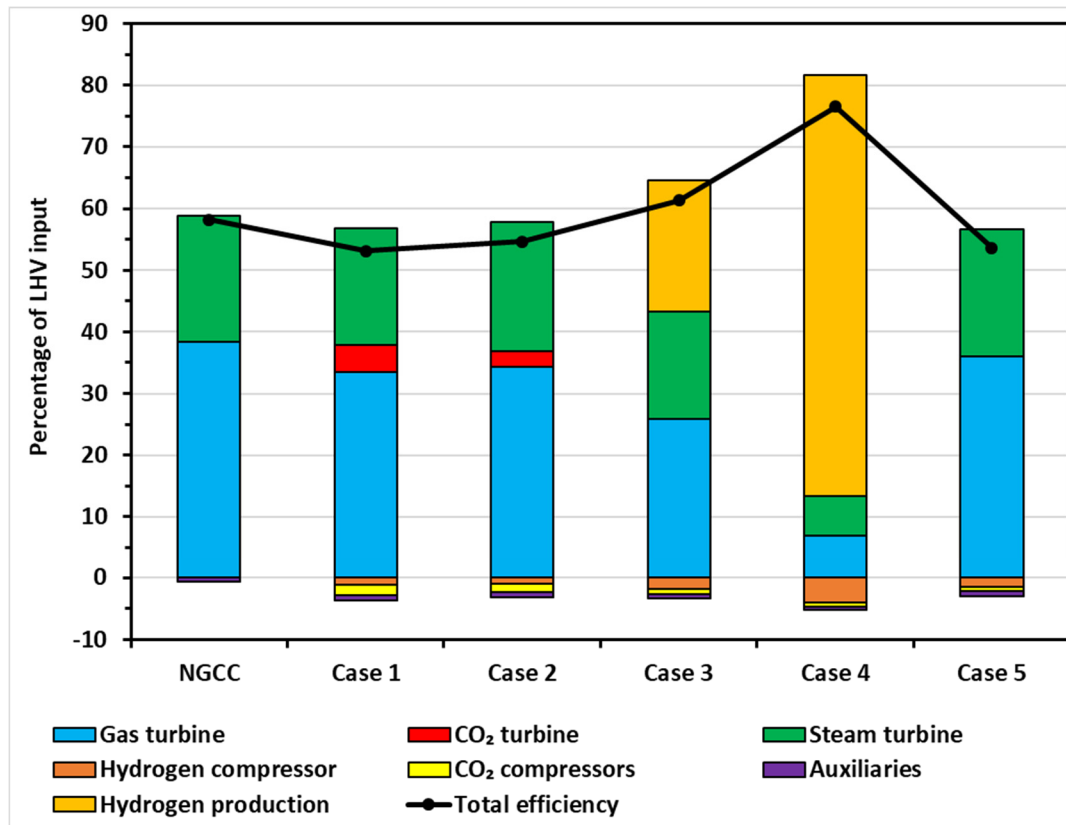

Figure 9. Power breakdown and total efficiency of the different cases.

With closer process coupling in case 2 (Figure 4), the heat integration scheme is substantially simplified, largely because no steam needs to be raised for the MA-CLR process (steam is supplied by the CLC fuel reactor outlet gases). Figure 8 shows that the net electrical efficiency obtained in this case is 54.62%, an improvement of ~1.54%-points. As shown in Figure 9, about 0.5%-points of this improvement come from a decrease in H_2 and CO_2 compression power and the remaining 1%-point from increased power generation from gas, steam, and CO_2 turbines. CO_2 compression duty is reduced to 0.24 MJ/kg-CO_2 because part of the CLC fuel reactor outlet gases is not expanded to atmospheric pressure (being fed to the MA-CLR process instead). The retentate stream from the MA-CLR is at 20 bar pressure and is therefore introduced in the CO_2 compression train in the third stage. On the other hand, this reduces the power production by CO_2 expander to 2.5% of LHV input. However, this 1.8%-point reduction in power output is more than compensated by a 0.9%-point increase in gas turbine power output and a 2%-point increase in steam turbine output. Due to the efficient integration of steam from the CLC fuel reactor, less heat is required in the MA-CLR plant, reducing its fuel consumption for a given hydrogen output and making more steam available to the steam turbine. When compared to the NGCC reference case, the energy penalty for case 2 is 3.55%-points (Figure 8). This mainly comes from the H_2/CO_2 compressors as the reduction in power production from the gas, CO_2 and steam turbines is only 0.98%-points.

In case 3 (Figure 5), the whole CO_2 outlet stream from the CLC plant is mixed with the NG feed to the MA-CLR plant so that excess H_2 can be produced while maintaining the steam-to-carbon ratio of 2.

As shown in Figure 8, the electrical efficiency obtained is only 39.92% due to the significant amount of hydrogen that is exported by this plant (hydrogen production efficiency of 21.36%). Power production is shifted more towards the steam turbines due to the substantial amount of heat that is made available to the MA-CLR reactors from the CLC reduction outlet, allowing more steam for power production to be raised in the MA-CLR plant. It can also be noted that hydrogen compression work increased due to significant hydrogen exports that require compression to 150 bar. On the other hand, CO_2 compression duty reduced because no CO_2 is expanded to atmospheric pressure in this case. The CO_2 in MA-CLR retentate is at 20 bar and require only one stage compression to reach supercritical state. As a result, the CO_2 compression energy is 0.15 MJ/kg-CO_2, a considerable reduction from previous cases. Hence, this case has no generation from a CO_2 turbine. The global electrical and H_2 production efficiencies are depicted in Figure 10, showing that the actual electric efficiency of this plant is similar to case 2. The global H_2 efficiency obtained is 68.09%, which is similar to a conventional SMR plant with CO_2 capture [22]. The overall energy efficiency obtained is 61.28% which falls between the NGCC and SMR plant energy efficiencies. When compared to NGCC reference case, the actual energy penalty in terms of electricity is 3.71%-points (Figure 8).
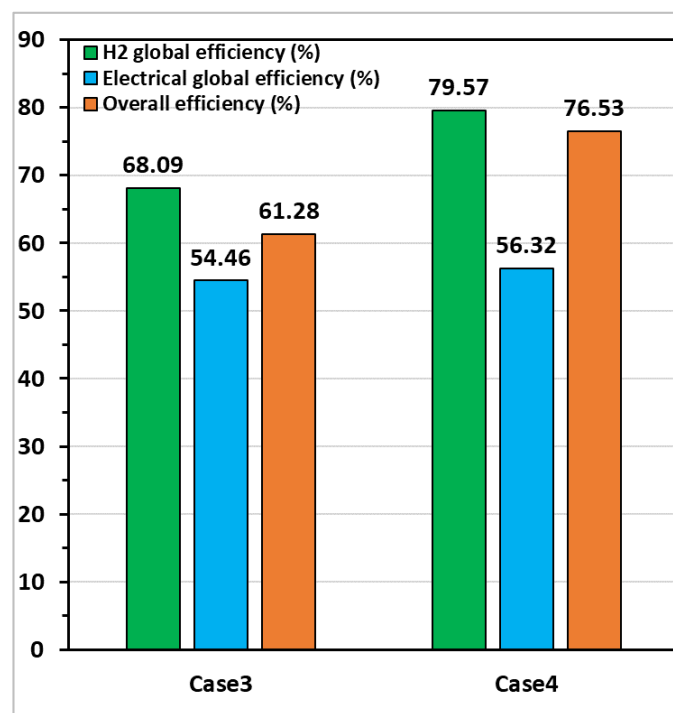

Figure 10. Performance of cases 3 and 4 producing both power and H_2 using Equations (6)–(8).

It can be noted that added firing up to the high TIT of modern gas turbines (~1600 °C) will shift the balance of energy output from the plant more towards electricity as more of the produced H_2 will be required in the added combustor to achieve the larger temperature increase of the depleted air stream from CLC. The good global electric efficiency of this plant suggests that integrated CLC and MA-CLR plants will remain attractive as the firing temperature of gas turbines keeps improving over the coming decades. It has been estimated in our previous work that, by using a state-of-the-art gas turbine with TIT 1550 °C, the energy penalty could be as low as 0.6% [33].

In case 4, the MA-CLR and CLC plants are combined to produce both power and H_2. As shown in Figure 8, this plant is mainly a hydrogen production plant with a net electrical efficiency of only 8.25%. It can also be noted from Figure 9 that the gas and steam turbines now produce almost similar power. Given that only a small fraction of the fuel heating value is converted to high-grade heat for generating power in the combined cycle, the steam that can be raised from cooling the large permeate stream substantially increases the relative contribution of the steam turbines. The H_2 compression work is

considerably larger due to the large amount of hydrogen exports, whereas the CO_2 compression work is low because the CO_2 stream is not expanded. The global electrical efficiency depicted in Figure 10 is 56.32% which gives an energy penalty of only 1.85%-points. This is a very good performance, but it can only be achieved when the plant operates mostly as a hydrogen production facility to efficiently utilize the large amount of steam available from the 2-phase flow heat exchanger for hydrogen production. Due to this efficient steam generation, the global H_2 production efficiency is also high at 79.57%, achieving parity with an SMR plant without CO_2 capture. The resulting overall efficiency obtained is 76.53%, which is 15.25%-points higher than that of case 3.

Stream information for this case is shown in Table 3. The 2-phase flow heat exchanger exchanges heat between streams 7 and 4, using some of the condensation enthalpy in the steam in stream 7 to raise steam in stream 4. It is shown that stream 7 has a slightly lower pressure and steam mole fraction than stream 4, meaning that the steam in stream 7 will start to condense at a lower temperature than the last steam in stream 4 will evaporate. Thus, not all the steam condensation enthalpy in stream 7 can be used to generate steam in stream 4, requiring the sensible heat to be used instead. For this reason, stream 4 could only be heated to 220 °C before introduction to the MA-CLR reactor (stream 5).

Similar to case 3, it can also be noted that the use of modern gas turbines with higher TIT will shift the energy output balance more towards power. The very high global electric efficiency of this plant suggests that such an integration will be highly attractive. However, an important limitation is that turbines with very high TIT generally have high power ratings, requiring the plant to produce a large power output. To utilize such a large-scale gas turbine, a greater share of output energy must go to power production than that observed for case 4 in Figure 9.

Case 5 illustrates an integration where case 4 can be modified for power production only. Instead of being sent to the main steam cycle, the steam produced by cooling the permeate stream is expanded to 6 bar and used as sweep gas in the Pd membranes to extract more heat from the reactor and increase the driving force for H_2 permeation. Figure 8 shows that the net electrical efficiency obtained is 53.63% with an energy penalty of 4.54%-points, which is about 1%-point more than case 2. This is largely because considerably more hydrogen needs to be produced and fed to the added combustor in this case due to the additional mass of the steam diluting the hydrogen fuel that must be heated up after the air reactor. Even though this integration achieves a high hydrogen production efficiency, producing heat via the CLC mechanism is still considerably more efficient than firing efficiently produced hydrogen, so a shift in heat release from the CLC reactor to the added combustor reduces plant efficiency. In addition, the H_2 compression duty for case 5 is 0.5%-points higher than for case 2 because of the larger H_2 flowrate that needs to be fed to the added combustor and the additional steam in this stream.

The CO_2 capture efficiency and CO_2 avoidance, in this case, are both 99.8%. This is slightly less than the previous cases due to the presence of large amount of water in the mixture (stream 8, Table 4) resulting in more solute CO_2 loss with the liquid water. Table 4 also shows that the steam content of stream 7 is considerably higher than it was in Table 3 due to the larger amount of NG that is combusted instead of being reformed. This allows the steam in this stream to start condensing at higher temperatures in the 2-phase flow heat exchanger. For this reason, most of the steam condensation enthalpy can be efficiently recovered to produce new steam in stream 5, preheating this stream to 650 °C in Table 4 instead of only 220 °C as shown in Table 3.

It will also be possible to develop a combination of the steam treatment in cases 4 and 5 by splitting the produced steam between the steam cycle and the membrane sweep. This will shift case 4 towards greater power production as required by large state-of-the-art gas turbines while improving on the efficiency of case 5.

Flexible operation should also be possible with these plants. In general, part-load operation of the gas turbine reduces the TIT, the pressure ratio, and the air flowrate. A lower TIT will require less added hydrogen firing, decreasing the energy penalty related to clean hydrogen production. This could allow more H_2 to be exported, but hydrogen production from the membranes will also decrease due to the lower pressure in the membrane reactor. This could be compensated to some degree by further

reducing the permeate pressure. More detailed studies at different gas turbine operating points will be required to better understand the potential for flexible power and hydrogen production from these highly efficient process integrations.

5. Conclusions

The current study deals with the efficiency improvement by process integration of a CLC plant and an MA-CLR plant. Such an integration solves the fundamental low turbine inlet temperature issue when using CLC technology for combined cycle power production. A hydrogen fired combustor is added after the CLC reactors to raise the CLC outlet temperature for achieving a specified TIT. If this hydrogen can be efficiently produced, such added firing can bring substantial efficiency gains.

Process integration for producing the hydrogen needed for added firing in a highly efficient manner was the primary focus of this study. The MA-CLR concept was identified as the most promising alternative for supplying this hydrogen. When the CLC and MA-CLR plants are operated independently in case 1, the energy penalty already reduces from around 8%-points for post-combustion CO_2 capture and CLC without added firing to 5.1% points. Closer integration by feeding some of the CLC fuel reactor outlet gases to the MA-CLR reactor as a steam supply in case 2 reduced the energy penalty to 3.6%-points.

When all the CLC fuel reactor outlet gases are used in the MA-CLR reactor in case 3, excess hydrogen can be produced. The equivalent net electric efficiency remained almost unchanged, but about a third of the plant energy output shifted to hydrogen produced with a reasonable equivalent efficiency of 68.09%.

Finally, the CLC and MA-CLR reactors were combined by operating the MA-CLR air reactor at the high air flowrates and temperatures needed by CLC. This integration was combined with a 2-phase flow heat exchanger that efficiently produced steam for reforming from the condensation enthalpy of the steam in the fuel reactor outlet stream. The first such plant integration (case 4) produced primarily hydrogen at a very attractive efficiency of 79.57%. Only about 11% of the useful plant energy output was power, also produced at high efficiency, resulting in an energy penalty of only 1.9%-points. Transitioning this plant to power production in case 5 only increases the energy penalty to 4.5%-points.

In conclusion, several promising process integrations were identified for overcoming the fundamental drawback of low TIT when using CLC for high efficiency combined cycle power production. These integrations can greatly reduce the energy penalty of CO_2 capture from natural gas-fired power plants while maintaining complete CO_2 avoidance. Further research is recommended.

Nomenclature

2P-HX	Two-phase heat exchanger
AC	Air compressor
AR	Air reactor
CC	Combined cycle
CCS	Carbon capture and storage
CLC	Chemical looping combustion
CLR	Chemical looping reforming
COMB	Combustor
COMP	Compressor
COND	Condenser

COT	Combustor outlet temperature
CT	Cooling tower
CWP	Cooling water pump
EBTF	European benchmark task force
ECO	Economizer
EGR	Exhaust gas recirculation
EVA	Evaporator
EX	Expander
FR	Fuel reactor
FW	Feed water
FWP	Feed water pump
GPSA	Gas processors suppliers association
GSR	Gas switching reforming
GT	Gas turbine
HC	Hydrogen compressor
HHV	High heating value
HP	High pressure
HRSG	Heat recovery steam generator
IP	Intermediate pressure
LHV	Low heating value
LP	Low pressure
MA-CLR	Membrane-assisted chemical looping reforming
NG	Natural gas
NGCC	Natural gas combine cycle
OC	Oxygen carrier
PCC	Post-combustion capture
PH	Preheater
RGIBBS	Reactor based on Gibbs energy minimization
RKS-BM	Redlich-Kwong-Soave-Boston-Mathias
SH	Superheater
SMR	Steam-methane reforming
ST	Steam turbine
TIT	Turbine inlet temperature

References

1. IPCC. *Fifth Assessment Report: Mitigation of Climate Change*; IPCC: New York, NY, USA, 2014.
2. UNFCCC Historic Paris Agreement on Climate Change. Available online: https://unfccc.int/process-and-meetings/the-paris-agreement/the-paris-agreement (accessed on 31 May 2019).
3. Diego, M.E.; Bellas, J.-M.; Pourkashanian, M. Techno-economic analysis of a hybrid CO_2 capture system for natural gas combined cycles with selective exhaust gas recirculation. *Appl. Energy* **2018**, *215*, 778–791. [CrossRef]
4. Ishida, M.; Zheng, D.; Akehata, T. Evaluation of a chemical-looping-combustion power-generation system by graphic exergy analysis. *Energy* **1987**, *12*, 147–154. [CrossRef]
5. Ishida, M.; Jin, H. CO_2 recovery in a power plant with chemical looping combustion. *Energy Convers. Manag.* **1997**, *38*, S187–S192. [CrossRef]
6. Naqvi, R.; Wolf, J.; Bolland, O. Part-load analysis of a chemical looping combustion (CLC) combined cycle with CO_2 capture. *Energy* **2007**, *32*, 360–370. [CrossRef]
7. Naqvi, R.; Bolland, O. Multi-stage chemical looping combustion (CLC) for combined cycles with CO_2 capture. *Int. J. Greenh. Gas Control* **2007**, *1*, 19–30. [CrossRef]
8. Hassan, B.; Ogidiama, O.V.; Khan, M.N.; Shamim, T. Energy and exergy analyses of a power plant with carbon dioxide capture using multistage chemical looping combustion. *J. Energy Resour. Technol.* **2016**, *139*, 032002. [CrossRef]

9.　Zhu, L.; He, Y.; Li, L.; Wu, P. Tech-economic assessment of second-generation CCS: Chemical looping combustion. *Energy* **2018**, *144*, 915–927. [CrossRef]

10.　Ogidiama, O.V.; Abu Zahra, M.; Shamim, T. Techno-Economic Analysis of a Carbon Capture Chemical Looping Combustion Power Plant. *J. Energy Resour. Technol.* **2018**, *140*. [CrossRef]

11.　Zerobin, F.; Pröll, T. Potential and limitations of power generation via chemical looping combustion of gaseous fuels. *Int. J. Greenh. Gas Control* **2017**, *64*, 174–182. [CrossRef]

12.　Ekström, C.; Schwendig, F.; Biede, O.; Franco, F.; Haupt, G.; de Koeijer, G.; Papapavlou, C.; Røkke, P.E. Techno-economic evaluations and benchmarking of pre-combustion CO_2 capture and oxy-fuel processes developed in the European ENCAP project. *Energy Procedia* **2009**, *1*, 4233–4240. [CrossRef]

13.　Petriz-Prieto, M.A.; Rico-Ramirez, V.; Gonzalez-Alatorre, G.; Gómez-Castro, F.I.; Diwekar, U.M. A comparative simulation study of power generation plants involving chemical looping combustion systems. *Comput. Chem. Eng.* **2016**, *84*, 434–445. [CrossRef]

14.　Porrazzo, R.; White, G.; Ocone, R. Techno-economic investigation of a chemical looping combustion based power plant. *Faraday Discuss.* **2016**, *192*, 437–457. [CrossRef] [PubMed]

15.　Consonni, S.; Lozza, G.; Pelliccia, G.; Rossini, S.; Saviano, F. Chemical looping combustion for combined cycles with CO_2 capture. *J. Eng. Gas Turbines Power* **2006**, *128*, 525. [CrossRef]

16.　Khan, M.N.; Shamim, T. Thermodynamic screening of suitable oxygen carriers for a three reactor chemical looping reforming system. *Int. J. Hydrogen Energy* **2017**, *42*, 15745–15760. [CrossRef]

17.　Baek, J.-I.; Ryu, J.; Lee, J.B.; Eom, T.-H.; Kim, K.-S.; Yang, S.-R.; Ryu, C.K. Highly attrition resistant oxygen carrier for chemical looping combustion. *Energy Procedia* **2011**, *4*, 349–355. [CrossRef]

18.　MHI Achieves 1,600°C Turbine Inlet Temperature in Test Operation of | Mitsubishi Heavy Industries, Ltd. Global Website. Available online: https://www.mhi.com/news/story/1105261435.html (accessed on 5 November 2018).

19.　Khan, M.N.; Cloete, S.; Amini, S. Efficiency Improvement of Chemical Looping Combustion Combined Cycle Power Plants. *Energy Technol.* **2019**, 1900567. [CrossRef]

20.　Khojasteh Salkuyeh, Y.; Saville, B.A.; MacLean, H.L. Techno-economic analysis and life cycle assessment of hydrogen production from natural gas using current and emerging technologies. *Int. J. Hydrogen Energy* **2017**, *42*, 18894–18909. [CrossRef]

21.　Khan, M.N.; Shamim, T. Techno-economic assessment of a chemical looping reforming combined cycle plant with iron and tungsten based oxygen carriers. *Int. J. Hydrogen Energy* **2019**, *44*, 11525–11534. [CrossRef]

22.　Spallina, V.; Pandolfo, D.; Battistella, A.; Romano, M.C.; Van Sint Annaland, M.; Gallucci, F. Techno-economic assessment of membrane assisted fluidized bed reactors for pure H2 production with CO_2 capture. *Energy Convers. Manag.* **2016**, *120*, 257–273. [CrossRef]

23.　Medrano, J.A.; Potdar, I.; Melendez, J.; Spallina, V.; Pacheco-Tanaka, D.A.; van Sint Annaland, M.; Gallucci, F. The membrane-assisted chemical looping reforming concept for efficient H2 production with inherent CO_2 capture: Experimental demonstration and model validation. *Appl. Energy* **2018**, *215*, 75–86. [CrossRef]

24.　Nazir, S.M.; Cloete, J.H.; Cloete, S.; Amini, S. Gas switching reforming (GSR) for power generation with CO_2 capture: Process efficiency improvement studies. *Energy* **2019**, *167*, 757–765. [CrossRef]

25.　Anantharaman, R.; Bolland, O.; Booth, N.; van Dorst, E.; Ekstrom, C.; Fernandes, E.S.; Franco, F.; Macchi, E.; Manzolini, G.; Nikolic, D.; et al. *DECARBit: European Best Practice Guidelines for Assessment of CO_2 Capture Technologies*; Norwegian University of Science and Technology: Trondheim, Norway, 2011.

26.　Thermoflow. *Thermoflex V26 User Guide*; Thermoflow: Southborough, MA, USA, 2017.

27.　Aspen Plus. *Aspen Plus V10 User Guide*; Version 10; Aspen Technology Inc.: Bedford, MA, USA, 2018.

28.　Cloete, S.; Khan, M.N.; Amini, S. Economic assessment of membrane-assisted autothermal reforming for cost effective hydrogen production with CO_2 capture. *Int. J. Hydrogen Energy* **2019**, *44*, 3492–3510. [CrossRef]

29.　Aspen Technology Inc. *Aspen Physical Property System*; Aspen Technology Inc.: Cambridge, MA, USA, 2006.

30.　GPSA. *Engineering Data Book*; Wiley-Blackwell: Hoboken, NJ, USA, 2004.

31.　Stull, D.R.; Prophet, H. *JANAF Thermochemical Data*, 2nd ed.; US National Bureau of Standards: Washington, DC, USA, 1971.

32. Ystad, P.A.M.; Bolland, O.; Hillestad, M. NGCC and hard-coal power plant with CO_2 capture based on absorption. *Energy Procedia* **2012**, *23*, 33–44. [CrossRef]

33. Khan, M.N.; Chiesa, P.; Cloete, S.; Amini, S. Integration of chemical looping combustion for cost-effective CO_2 capture from state-of-the-art natural gas combined cycles. *Energy Convers. Manag. X* **2020**, *7*, 100044. [CrossRef]

34. Jackson, S.; Brodal, E. Optimization of the energy consumption of a carbon capture and sequestration related carbon dioxide compression processes. *Energies* **2019**, *12*, 1603. [CrossRef]